Journal of the Physical Society of Japan **84**, 121013 (2015)
http://dx.doi.org/10.7566/JPSJ.84.121013

Chemical Vapor Deposition Growth of Graphene and Related Materials

Ryo Kitaura[1], Yasumitsu Miyata[2], Rong Xiang[3], James Hone[4], Jing Kong[5], Rodney S. Ruoff[6], and Shigeo Maruyama[3,7]

[1]*Nagoya University, Nagoya 464-0814, Japan*
[2]*Tokyo Metropolitan University, Hachioji, Tokyo 192-0397, Japan*
[3]*The University of Tokyo, Bunkyo, Tokyo 113-8656, Japan*
[4]*Columbia University, New York, NY 10027, U.S.A.*
[5]*Massachusetts Institute of Technology, Cambridge, MA 02139, U.S.A.*
[6]*Center for Multidimensional Carbon Materials (an IBS Center) and Department of Chemistry, Ulsan National Institute of Science and Technology, Ulsan 689-798, Republic of Korea*
[7]*National Institute of Advanced Industrial Science and Technology (AIST), Tsukuba, Ibaraki 305-8564, Japan*

(Received May 14, 2015; accepted June 30, 2015; published online November 11, 2015)

Research on atomic layers including graphene, hexagonal boron nitride (hBN), transition metal dichalcogenides (TMDCs) and their heterostructures has attracted a great deal of attention. Chemical vapor deposition (CVD) can provide large-area structure-defined high-quality atomic layer samples, which have considerably contributed to the recent advancement of atomic-layer research. In this article, we focus on the CVD growth of various atomic layers and review recent progresses including (1) the CVD growth of graphene using methane and ethanol as carbon sources, (2) the CVD growth of hBN using borazine and ammonia borane, (3) the CVD growth of various TMDCs using single and multi-furnace methods, and (4) CVD growth of vertical and lateral heterostructures such as graphene/hBN, MoS_2/graphite, WS_2/hBN and MoS_2/WS_2.

1. Introduction

The recent progress of research on atomic layers including graphene, hexagonal boron nitride (hBN), and transition metal dichalcogenides (TMDCs) has reinvigorated the study of atomic layers. Reports on graphene can be traced back to early work in the 1960's with identification of "monolayer graphite" (i.e., graphene) in 1969,[1,2] while the first isolation of graphene on insulating substrates in 2005 has led to the observation of fascinating electronic properties of graphene, igniting intense interest in a wide range of possible applications and further research on its basic properties.[3–8] Atomic layers have been studied in terms of colloidal science and through chemical exfoliation, and now there is intense interest in their physical properties and possible role in various applications.[9] In addition to individual atomic layers that have been investigated so far, atomic layer heterostructures are being developed.[4,10,11] Various atomic layers and their unique properties have been providing a widespread platform to open up novel chemistry and physics in two dimensions.[5,12]

The progress of materials science and condensed matter physics relies on the development of sample preparation methods, and the research on atomic layers is no exception. The preparation of atomic layer samples can be performed by bottom-up or top-down methods. By revisiting a known method of repetitive peeling with adhesive tape that was, for example, reported in the 1960s for the preparation of ultrathin samples of layered materials such as metal chalcogenides,[13] graphene was isolated on an insulating substrate as reported in 2005; this method has been referred to as "mechanical exfoliation". The preparation of monolayer flakes of graphene, hBN, and TMDCs has been achieved by this top-down method,[4,14–16] and the finding of massless Dirac fermions in graphene, the observations of quantum Hall and fractional quantum Hall effects in graphene, the realization of high-performance FETs by TMDCs, and the optical control of the valley degree of freedom in TMDCs, etc., have also been accomplished with samples prepared by "tape peeling", i.e., mechanical exfoliation.[4,17–19]

Although there have been significant contributions from the top-down method, bottom-up methods, such as chemical vapor deposition (CVD), are indispensable in atomic layers research. The advantages of the CVD growth of atomic layers are roughly summarized as follows: the realization of large-area atomic layers, layer-number selectivity, and the direct growth of vertical and lateral heterostructures. The use of large-area flakes facilitates device fabrication, leading to the more straightforward investigation of the physical and chemical properties of atomic layers. In addition, large-area samples are essential, in particular, in terms of device applications, because semiconductor device applications usually need wafer-size crystals. The layer-number selectivity is another advantage of CVD growth. Because physical properties strongly depend on the number of layers, layer-number-selective preparation (particularly monolayer preparation) is crucial in atomic layers research.[20] The exfoliation-based method, however, provides flakes with various layer numbers, and finding monolayers, bilayers, and so forth is a time-consuming task. Finally, the growth of heterostructures is a significant advantage of the CVD method. Even though vertical heterostructures can be prepared by the transfer-based manual stacking method,[21] the direct CVD growth of vertical heterostructures is an important issue. In the case of the transfer-based manual stacking method, obtaining a clean interface between layers is not easy, and bubble formation and contamination are significant problems in the preparation of high-quality vertical heterostructures. In contrast, the direct CVD growth of heterostructures can provide high-quality heterostructures with clean interfaces because heterostructures are directly grown through a high-temperature dry process.[22–25] In addition, the preparation of lateral heterostructures by transfer-based methods is, in principle, impossible and can be prepared only by the CVD method. The advantages shown above are absent in the top-down

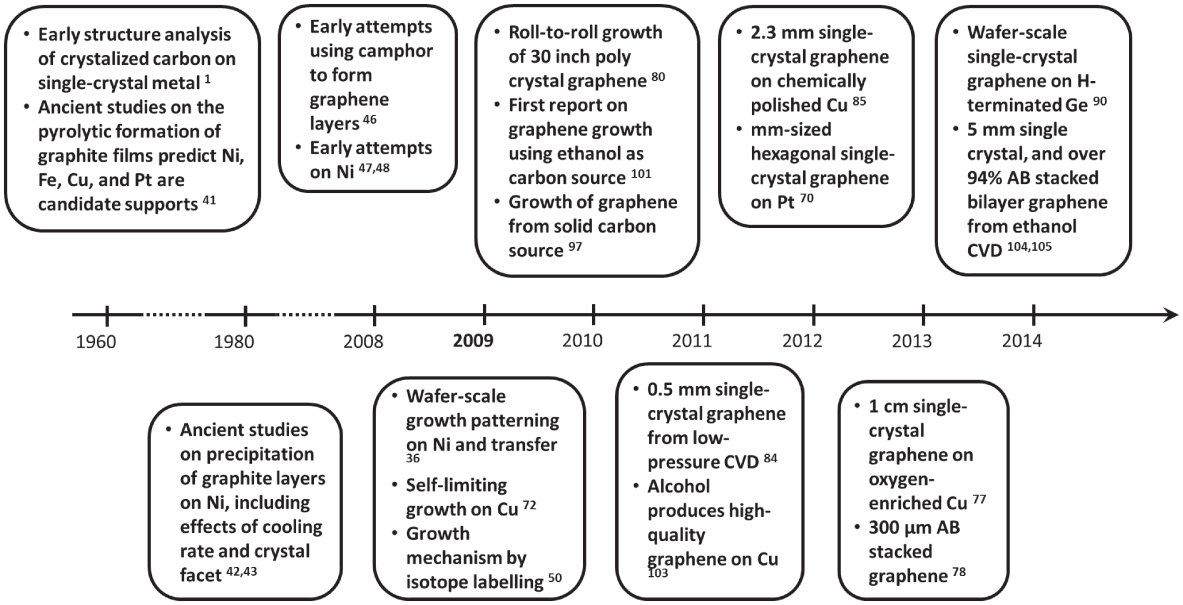

Fig. 1. Timeline of selected progress in CVD synthesis of graphene from methane and ethanol.

method, making the CVD growth indispensable in atomic layers research.

In this review article, we focus on the CVD growth of atomic layers including graphene, hBN, TMDC and atomic-layer heterostructures. In Sect. 2, the CVD growth of graphene, in particular, using methane and ethanol as carbon sources, is presented. The CVD growth of hBN is then discussed briefly in Sect. 3. In Sect. 4, bottom-up approaches to the growth of TMDC atomic layers using one-furnace, multi-furnace CVD and molecular beam epitaxy (MBE) are discussed. In Sect. 5, the growth of vertical and lateral heterostructures including graphene/hBN, TMDC/graphene, TMDC/hBN, and TMDC/TMDC is presented.

2. CVD Growth of Graphene

2.1 CVD growth of graphene

Although the term "graphene" appeared and was even standardized in 1986,[3,26] its deposition on insulating substrates ignited its research in the past decade.[27,28] Driven by its superior properties and therefore potential applications,[6,29–34] as well as the unprecedentedly rich physics,[4,8] significant effort has been made to obtain or synthesize graphene in a controlled manner. Methods including mechanical exfoliation,[3] thermal decomposition of SiC,[7] chemical exfoliation,[35,36] and CVD[37,38] have been used to produce graphene. Each of these methods has its own advantages and disadvantages, so in principle, the preparation strongly depends on the final use of graphene product. CVD is, however, undoubtedly the most widely investigated method so far,[39] owing to its potential in large-scale production, just as been demonstrated in study of carbon nanotubes (CNT).[40] Indeed, there are a lot similarities in mechanisms of graphene and CNT growth, and initial attempts of the graphene CVD inherited not only recipes but also research methodologies from CNTs, particularly single-walled carbon nanotubes (SWNTs).[40] However, recent fast development of graphene synthesis has made graphene growth *very different* from conventional CNT growth. Some of the new findings on graphene formation can perhaps provide feedback about the growth mechanism of CNTs, and may even facilitate the controlled growth of CNT, as will be discussed in detail in the following sections. Selected events in the CVD synthesis of graphene from methane and ethanol are summarized in Fig. 1.

2.2 Polycrystal graphene

The growth of monolayer graphene over transition metals occurred many years prior to the isolation of graphene in 2004.[3] For instance, Banerjee et al. investigated the pyrolytic formation of graphite films on Ni, Cu, and Pt from carbon suboxide (C_3O_2), and showed variations in the growth rate and thickness of the films.[41] They noted that

> "*In particular, substrates of nickel and iron are of interest. They are highly active catalysts for the decomposition of carbonaceous gases, apparently because of the incomplete filling of their 3d bands. In addition, they markedly increase the crystallinity of the carbon formed as decomposition product.*"

A similar work can also be found in the research of Blakely and coauthors in 1970–80s, when they reported a series of work on the surface segregation of mono- and multilayers of graphene on Ni, Pt, Pd, and Co.[42,43] They even studied the influence of crystal orientation on growth, which has also been investigated during the past decade by many groups.[44,45]

Besides these studies of graphene growth by surface scientists, the modern CVD synthesis of graphene has followed a trajectory from synthesis of multilayer films with inconsistent layer numbers as a function of lateral position in the film to the more controlled synthesis of monolayer only. Early attempts include reports by Somani et al.,[46] Obraztsov et al.,[47] and Yu et al.[48] All these early attempts resulted in a few to few tens of layers of graphene with varying thickness across the film. One work that opened the way for graphene application in electronics was performed by Kim et al. in

2009, who achieved the CVD growth of wafer-scale graphene and presented a versatile strategy for transferring graphene onto a different substrate.[37] Their work, as well as subsequent studies by other groups,[38,49] opened the practical utilization of graphene as a new material from laboratory research to industrial application.

Before 2009, the most studied metal substrate for graphene synthesis was Ni. However, Ni generally suffers from the difficulty in precise control over the thickness of the obtained material. Usually, the product contains both mono- and multilayer graphene. This is attributed to the high solubility of carbon in Ni. By precipitation from the bulk Ni to the surface, the extra growth of the graphitic film occurs during cool-down (as discussed further below).[50] Many strategies have been proposed to increase the proportion of mono-layer graphene. Controlling the cooling rate, surface morphology, growth reagents, and adopting low pressures and temperatures, have all been proven to be capable of increasing the proportion of the monolayer in the product.[38,51,52]

In parallel, many other metals were proposed as candidates to support graphene growth. Graphene has been synthesized on Ru,[53,54] Co,[55] Pd,[56] Rh,[57] Au,[58] Pt,[59] and other metal substrates,[60,61] although the "processing window" varies from metal to metal. One thoroughly studied metal is Ru. Ru has a hexagonal closest packed structure, and low carbon solubility, and easily form a crystalline surface at high temperatures. These properties make single crystal Ru a good choice for the epitaxial formation of graphene, and high-quality mono- and bilayer graphenes have been successfully synthesized on Ru (0001) surface.[62,63] Since many experiments have been performed in UHV, the structure of graphene on Ru and thus the metal–graphene interface, have also been studied.[64–67] Pt is another metal that has been well studied for graphene growth.[59,68,69] Large mono- and bilayer graphenes can be formed on both single- and polycrystal Pt at ambient pressure. The Cheng group also demonstrated that transfer of graphene from Pt to another substrate is feasible through a bubble-assisted transfer, in which the Pt substrate can be repeatedly reused for growth and transfer.[70] Another approach is the use of metal alloy, and the Liu group stated that an alloy of Ni-Mo yielded 100% monolayer coverage.[71]

While many metals have been used for monolayer or multilayer growth, Cu has been the metal most frequently used including for scaled-up production,[72] as will be discussed in the next section. (Figure 2 shows graphene grown on Cu.)

One of the most significant advantages of Cu is its robustness. On all other different metals, there are usually narrow windows that monolayer graphene can form so it is not always "easy" to find the right conditions for growing monolayer graphene, while on Cu, in most cases, it is fairly "difficult" to form a second layer. This is normally called a self-limiting process, which is now understood to be due to the ultralow solubility of carbon in Cu and therefore from a surface-mediated growth mechanism.[50] The different mechanism between Ni and Cu was successfully demonstrated by isotope labeling; we note that isotope labeling has also been used in CNT research.[73–75] At the same time, the formation of graphene on Cu seems to be less sensitive to the Cu crystal orientation (many subsequent studies show that growth can readily span grain boundaries of Cu without affecting itself).[76–79] Together with its easy accessibility and low cost, Cu (mainly foil) has evidently become the most successful metal template and has opened a new generation of graphene CVD. Numerous exciting breakthroughs including the roll-to-roll growth of 30 inch graphene,[80] the growth of graphene with single crystals up to the cm scale,[77] and the new development of growth on Cu(111) foil.[81,82] Considering the explosive development of Cu-based CVD, instead of reviewing the complete history of graphene growth by Cu-based CVD, we will focus on the recent progress in the synthesis of large graphene single crystals, which has generated considerable interest over the past four years.

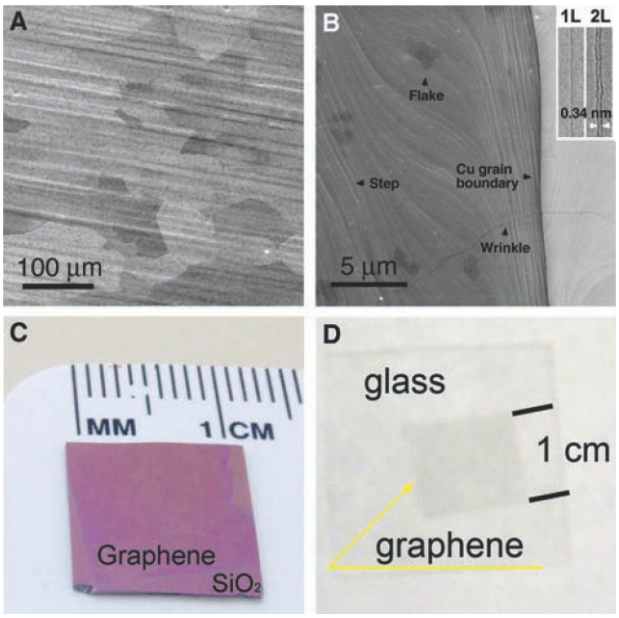

Fig. 2. (Color online) (A, B) SEM images of graphene grown on a Cu foil. (C, D) Optical microscopy image of graphene transferred onto a SiO_2/Si substrate and a glass plate, respectively. Reproduced from Ref. 72.

2.3 *Larger graphene single-crystals*

Initially, graphene films synthesized on Cu were polycrystals, with typical graphene single-crystal domain sizes of about tens of micrometers.[72] The grain boundaries in these films decrease both the electrical and mechanical qualities of graphene films.[79,83] Driven by the superior properties of structurally perfect graphene films, since 2011, efforts have been directed towards enlarging the single-crystal graphene domains up to the millimeter and even the centimeter scale.

Among major progresses of optimizing CVD conditions to realize the synthesis of millimeter-scale single-crystal graphene, several factors have been considered crucial. First, using a low partial pressure of the carbon precursor (which typically has been methane) significantly increases the chance of obtaining large single crystals. The Ruoff group reported that, at low flow rates and partial pressures of methane, single-crystal graphene flakes as large as 0.5 mm could be synthesized.[84] Following this pioneering work, many other research groups obtained millimeter-size graphene using a methane partial pressure as low as several Pa. Second, smoothing and cleaning the Cu foil surface, either by electropolishing or long-term annealing, or melting followed by resolidification, can reduce the nucleation density through the decrease in the number of preferred nucleation sites.[85,86]

Third, some techniques such as using Cu foil pockets or enclosures, Cu foil tubes, or Cu foil sandwiches are believed to contribute to the smoothing of the foil surface, slowing down the evaporation of Cu, and thus preventing contamination, which can increase the size of single crystal graphene regions formed inside these enclosed spaces.[84] Chen et al. showed that, by combining the strategies of low-partial-pressure methane, very smooth Cu surfaces, and Cu pockets or Cu tubes, graphene single crystals as large as 2 mm can be synthesized.[76] Recent results reveal that a small amount of oxygen, produced, for example, by using an oxygen-rich Cu foil or by deliberately introducing oxygen directly into the growth chamber, increases the growth rate and final size of the obtained graphene single crystals.[77,78,87] Graphene single crystals of cm-scale diameter were obtained through the selective use of oxygen with the Cu foil.

Behind these techniques that were adopted to increase the size of graphene single crystals, the key is to decrease the density of nucleation sites. Comparing the growth rates of graphene reported in the past five or six years, one may easily observe that the growth rate has not increased many-fold. In 2009, the grow rate was about ~6 μm/min as revealed by isotope labelling,[50] while in 2013, 1-cm-diameter graphene was obtained in a 12 h CVD at a growth rate of ~7 μm/min.[77] However, the nucleation density nowadays is many orders of magnitude decreased compared with the first report on Cu (10^4–10^5 vs 0.01 mm^{-2}). At this stage, nucleation generally randomly occurs on the foil. In this sense, controlling the precise growth density through, for example, site selective growth techniques,[79] may be an important step to further enlarge graphene single crystals. At the same time, unlike the growth of SWNTs that usually decelerates after a short time (usually called catalyst deactivation),[88,89] the factors that limit graphene growth are, in many case, technical issues, e.g., the evaporation of Cu after a long CVD time. It might be forecasted that relatively high growth rates are needed for larger graphene single crystals.

There is another strategy that has recently been proposed by Lee et al., who claimed that wafer-scale wrinkle-free single-crystal graphene can be obtained on silicon using a hydrogen-terminated germanium buffer layer.[90] Unlike on Cu foil where graphene has more than one dominant orientation preference,[45,79,91] graphene flakes formed on this substrate have identical orientations and finally merge into single crystals without apparent grain boundaries (although the sizes of initially formed grains were only few micrometers). Also, the authors claimed that the weak interaction between graphene and the underlying hydrogen-terminated germanium surface enabled the facile etch-free dry transfer of graphene and the recycling of the germanium substrate for continual graphene growth. Prior to this work it was found that graphene islands (domains) formed on Cu(111) have identical orientations.[81,92] More recently, the "seamless stitching" of graphene domains was discussed and 4×6 cm^2 single crystal graphene was presented as obtained on polished copper (111) foil.[82]

2.4 *Recent progress in ethanol CVD*

In the previous studies on graphene CVD, the widely used carbon source is methane.[40,72] The choice of methane was due to its stability at high temperatures as it was perceived that high temperatures might favor higher quality graphene.[72] However, for future industrial production, other alternative carbon sources, particularly those in liquid form at room temperature, may be used owing to their easier storage and transport. Also, it remains fundamentally interesting how different carbon sources influence graphene formation.

Indeed, since 2009, many other hydrocarbons and carbon-containing materials in gas,[93,94] liquid,[95,96] and solid states,[97–99] have all been proven to be at least effective for forming graphene. One of the most promising candidates, as proposed by Maruyama et al., in 2002 for the CVD growth of SWNTs, is ethanol.[100]

Ethanol is known as a cheap, clean, nontoxic liquid, which has been proven to be one of the most efficient carbon sources for the growth of SWNTs.[100] The oxygen in its molecular skeleton etches the less stable amorphous carbon by-product and therefore results in impurity-free SWNTs. For graphene growth, the recent discovery that oxygen is helpful for increasing the growth rate of graphene and passivating the excessive nucleation perks more interest.[77]

The first graphene CVD using ethanol as a carbon source was achieved soon after the first report on the CVD growth of graphene. In 2010, Miyata et al. synthesize monolayer graphene on Ni using ethanol as the carbon source in the ambient pressure CVD.[101] Later, in 2011 Guermoune et al., performed a more systematic experiment using alcohols, namely methanol, ethanol, and propanol, and obtained high-purity monolayer graphene in all three alcohols.[102] The mobility of the obtained graphene was around 2000 $cm^2\,V^{-1}\,s^{-1}$. In 2013, Zhao et al. further studied the growth behavior of graphene from ethanol on different facets of Cu and concluded low-index Cu facets of Cu(111) and Cu(100) play a critical role in the following self-limiting process of a continuous graphene sheet, whereas the Cu(110) and high-index facets favor the nucleation and formation of secondary layers.[103] High quality graphene form on Cu at a relatively low temperature 800 °C. More recently, Chen et al. have produced monolayer graphene single crystals up to 5 mm, which is on the same order of magnitude as those obtained from methane.[104] In general, although not as widely used presently as methane, ethanol seems to possess the same capability of producing monolayer graphene, regardless of the quality or size of the obtained graphene crystal.

At the same time, some differences between ethanol and methane were also observed in these studies. For example, in their first report, Miyata et al. believed that via flash cooling graphene was formed on Ni by a nonsegregation mechanism.[101] Zhao et al. further confirmed that ethanol followed a nonsegregation mechanism by isotope labelling.[103] Zhao et al. recently found that ethanol is also capable of producing bilayer graphene, within which over 94% of the layers are Bernal-stacked.[105] One interesting phenomenon observed here is that bilayer growth follows a layer-by-layer epitaxy mechanism, and a continuous substitution of graphene flakes occurs in the as-formed graphene (first layer), which is significantly different from previous observations in methane CVD.[106,107] The existing oxygen in ethanol may have played an important role in the growth, particularly in the etching and substitution of carbon atoms in the as-formed graphene, although further study is still needed to verify the role of

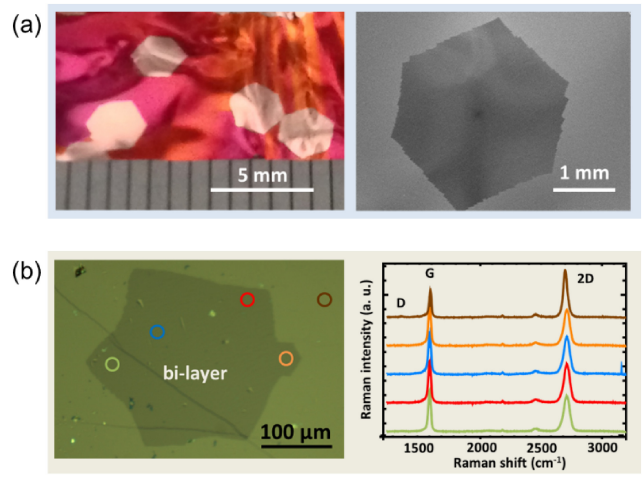

Fig. 3. (Color online) Mono- and bilayer graphenes synthesized from ethanol: (a) optical image of mm-scale single-crystal monolayer graphene on Cu and SEM image of the sample transferred onto SiO_2 substrate; (b) optical image of a 300 μm AB-stacked bilayer graphene synthesized and its corresponding Raman spectra.

oxygen. Nevertheless, ethanol has proven its potential in the controlled CVD synthesis of polycrystal graphene, large single crystal monolayer graphene, and AB-stacked bilayer graphene. Some representative graphene samples recently obtained by ethanol CVD are shown in Fig. 3.

3. CVD Growth of Hexagonal Boron Nitride

The development of graphene growth technique has also stimulated researchers to apply the same approach to the growth of other two-dimensional materials. Atomic layers of hBN are a representative sample. Even though the synthesis of the hBN bulk crystal has a long history, here, we focus our attention to recent progresses of the CVD growth of hBN atomic layers on metal substrates. Similarly to the CVD growth of graphene, mono- and few-layer hBN can be grown on the surfaces of similar metal substrates such as Ni, Co, Ru, Pt, and Cu.[108–117] As the precursors of hBN, ammonia borane (BNH_6, borazane),[108–112] borazine ($B_3N_3H_6$),[113–116] and the combination of ammonia and diborane[117] are used in place of methene and ethanol for graphene. Even though these hBN sources are solid or solution at room temperature, these compounds are easily evaporated by moderate heating and thus can be used for CVD growth under ambient and low-pressure conditions. In terms of stability under ambient condition, ammonia borane CVD can be conducted with a simple setup for laboratory experiments.[108–112] In the same manner as graphene, the growth of micrometer-sized monolayer hBN crystals was achieved on Cu and Co substrates (Fig. 4).[108,110] This indicates that these metal substrates have similar catalytic effects and solubilities for boron and nitrogen atoms as observed for carbon atoms on Cu.

Despite such success with the methodology developed in graphene studies, there are still several issues to be resolved for the practical use of CVD-grown hBN. First, current CVD techniques still lack a production method for a high-quality and perfectly uniform multilayer of hBN, which is highly required as an atomically flat and ultraclean dielectric layer for application in electronics. To date, the high carrier mobility of graphene has been realized using bulk hBN single

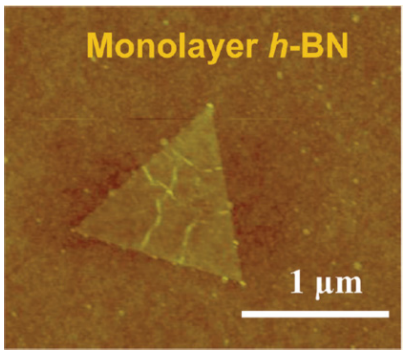

Fig. 4. (Color online) Atomic force microscopy image of a trigonal monolayer hBN grain grown on Cu foil. Reproduced from Ref. 110.

crystals grown in solutions such as barium boron nitride and nickel molybdenum.[118,119] Furthermore, the grain size of CVD-grown hBN has been limited to several tens of micrometers unlike CVD graphene.[110] The grains of the hBN crystal become trigonal because of the threefold symmetry of the crystal lattice. Long-time growth leads to the formation of continuous films with grain boundaries where pentagon–heptagon (5/7) defects were observed.[120] This may result in the degradation of intrinsic electric and mechanical properties. As reviewed in the heterostructure section, applications using hBN highly require the combination of hBN with other two-dimensional materials. Therefore, it is still highly desired to develop a technique for directly growing hBN on other two-dimensional materials.

4. CVD Growth of Transition Metal Dichalcogenides

Important early experiments on TMDCs have been performed using samples exfoliated from bulk crystals. For example, the first investigation of the FET properties of monolayer MoS_2 showing a high on/off ratio ($\sim 10^8$) and the first demonstration of intense PL emission from monolayer MoS_2 have been performed using MoS_2 samples prepared by exfoliation.[10,18] These pioneering works have ignited intense research interest toward TMDCs, and the following important works on TMDCs, such as the optical control of valley polarization and the observation of the valley Hall effect, have been urged to appear; these works have also been performed using the samples prepared by exfoliation. In addition to a sizable bandgap larger than 2 eV, the optical control of the valley degree of freedom is lacking in graphene, and the experimental observation of the valley-related physics has clearly demonstrated that TMDC is a promising post-graphene material.[121–124] Although exfoliated samples have been playing an important role in TMDC research, the CVD growth of TMDCs has attracted much attention. As discussed in the introduction section, the advantages of CVD growth are summarized as follows: the realization of large-area atomic layers, layer-number selectivity, and the direct growth of vertical and lateral heterostructures. The selective formation of a monolayer is an important advantage of the CVD growth of TMDCs because direct bandgap and valley-related properties can be seen particularly in the monolayer.[122] In addition, recent reports on the direct CVD growth of TMDC heterostructures (discussed in the next section) have also makes the CVD growth of TMDCs indispensable in TMDC research.

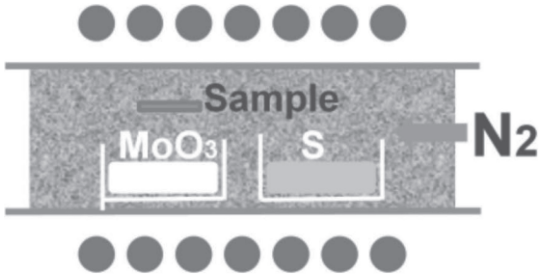

Fig. 5. Schematic diagram of single-furnace method for growth of MoS_2 from MoO_3 and elemental sulfur. Reproduced from Ref. 125.

The CVD growth of TMDCs can be roughly divided into two types: single-furnace and multi-furnace methods. The single-furnace method is the simplest method and has firstly reported.[125)] Figure 5 shows a schematic diagram of the single-furnace method to grow MoS_2 atomic layers. In this method, the metal source (MoO_3) and elemental sulfur are placed in a quartz reactor heated at 650 °C, leading to the vaporization of both MoO_3 and sulfur to grow MoS_2 flakes on a substrate placed nearby; in this case, SiO_2/Si substrates were used. TMDCs can be directly grown onto insulating substrates such as SiO_2/Si, sapphire, mica, and hBN because the CVD growth of TMDCs does not require catalytic action, which is different from those for graphene and hBN. Using the single-furnace method, large-area monolayer MoS_2, whose grain size is larger than 100 μm (Fig. 6), has been prepared.[126)] Note that carefully cleaned substrates are an important factor of large-area high-crystallinity MoS_2 growth. The grown MoS_2 flakes have various shapes including triangle, hexagonal and star-shape; triangular is the most frequently observed crystal shape of CVD-grown TMDCs.[127)] The formation of triangular MoS_2 is different from that of CVD-grown graphene, owing to the preferential formation of zigzag edges composed of metal or chalcogen during the CVD growth. When the surface coverage increases, MoS_2 grains merge to form a large-area single sheet, where grain boundaries such as 8–4–4 and 5–7 exist (Fig. 6).[126)]

Even though the single-furnace method is a simple and facile preparation technique for monolayer MoS_2, the application of this method to the preparation of other types of TMDCs is not feasible; this method needs a metal source that can vaporize at the growth temperature of TMDCs (typically around 700 °C). It is, in principle, possible to increase growth temperature to prompt the vaporization of metal sources, but, in this case, chalcogen immediately vaporizes before the formation of TMDCs. MoO_3 is a suitable metal source with sufficiently low sublimation temperature, and the single-furnace method with MoO_3 as a metal source has been utilized as a facile growth method for MoS_2 atomic layers.[128)] Another possible metal source is metal chloride that vaporizes well below the growth temperature. However, metal chlorides such as $MoCl_6$ and WCl_6 are very sensitive to moisture in air and readily decompose to produce HCl; these metal sources are not easy to handle.

This problem can be solved using the multi-furnace method. In this approach, chalcogen vaporization and TMDC growth (and/or metal source vaporization) can be performed at different temperatures, and TMDC growth can be maintained at high temperatures (~1000 °C) with the continuous supply of chalcogen. This method can be applied not only to Mo but also to other metals, leading to the growth of TMDCs including MoS_2, WS_2, $MoSe_2$, WSe_2, and so forth.[129–134)] In this method, metal sources can be vaporized during the growth or deposited prior to sulfurization. WO_3, for example, is thermally evaporated to deposit on a substrate, which is followed by sulfurization under sulfur flow at high temperatures. Large-area WS_2 films (~1 cm^2) have been prepared through this procedure (Fig. 7).[135)] WO_3 can also be supplied by vaporization, where the substrate and WO_3 are put in a furnace heated at a high temperature and sulfur is supplied upstream under buffer gas flow.[136,137)] This has also produced large-area monolayer WS_2, and it is reported that the grown monolayer WS_2 shows ambipolar FET characteristics with an ionic liquid top gate. Similarly, large-area monolayer WSe_2 has been grown using WO_3 and selenium as a metal source and chalcogen. The grown WSe_2 shows ambipolar characteristics and a high hole mobility of 90 $cm^2 V^{-1} s^{-1}$.[133)] The three-furnace method has also been

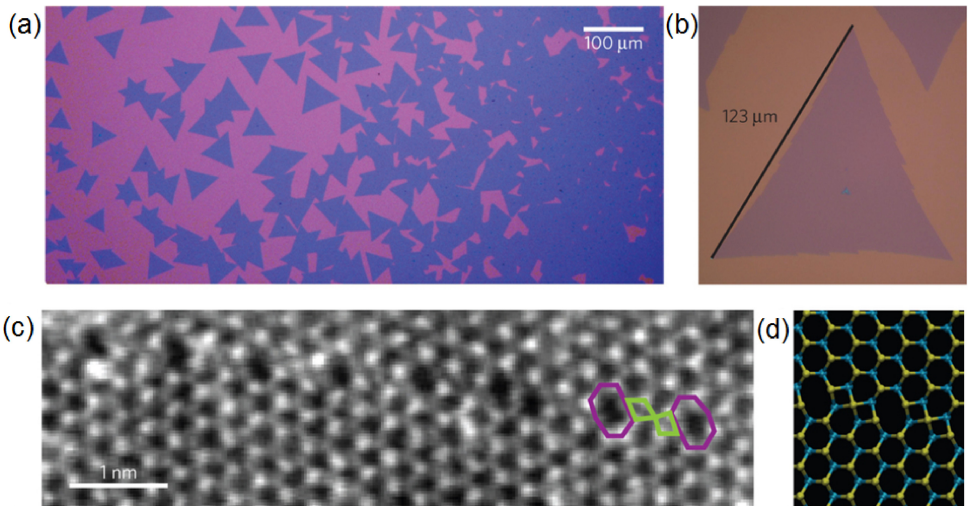

Fig. 6. (Color online) (a, b) Optical microscopy images of MoS_2 grown on SiO_2/Si substrates. Triangular MoS_2 crystals are seen as blue contrasts. (c, d) An atomic resolution TEM image and corresponding structure model of a grain boundary of grown MoS_2. Reproduced from Ref. 126.

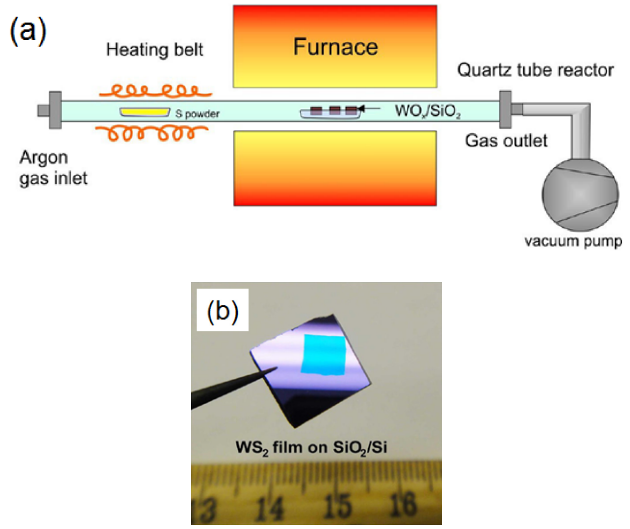

Fig. 7. (Color online) (a) Schematic presentation of CVD growth of WS_2 with two independent heating systems. The growth of WS_2 and the supply of sulfur are separated in this method. (b) Grown large-area WS_2 film on SiO_2/Si substrate. Reproduced from Ref. 135.

reported, where a metal source, chalcogen, and a substrate can be independently heated using three independent furnaces. The independent control of each source and the substrate contributes to the controlled growth of high-quality TMDCs, and the grown WS_2 on hBN shows the sharp photoluminescence peak (FWHM 25 meV at 2.01 eV) at room temperature.[24)]

Molecular beam epitaxy (MBE) is another bottom-up approach for the growth of various semiconductor thin films. MBE has been widely used as a highly controllable method of preparing thin films: the application of MBE to TMDCs is however still limited. Early studies on the MBE growth of TMDCs have been reported around 1990 by the Koma group. In their work, they have grown $MoSe_2$ and $NbSe_2$ in a UHV chamber (8×10^{-9} Pa), where the metal source and Se were evaporated by an electron beam evaporator and a Knudsen cell, respectively.[138)] They have also demonstrated the growth of vertical TMDC heterostructures by the direct MBE growth of a TMDC layer onto another TMDC layer, which they call van der Waals epitaxy.[139)] Similarly, $MoSe_2$ and $HfSe_2$ have recently been grown by MBE, and the electronic structure of MBE-grown $MoSe_2$ has been investigated by scanning tunneling microscopy.[140,141)] From the results of the scanning tunneling spectroscopy of MBE-grown monolayer $MoSe_2$, the single-particle electronic gap of monolayer $MoSe_2$ has been determined as 2.18 eV, and the exciton binding energy of 0.55 eV has also been determined as the energy difference between the single-particle gap and optical gap.[141)] Although the MBE growth of TMDCs has not been investigated very well, MBE has potential for growing high-quality TMDCs and heterostructures in a controlled way, which is expected to contribute to the elucidation of fundamentals of TMDCs and future applications; MBE can precisely control the supply rates of metal and chalcogen, allowing for the consecutive growth of heterostructures.

5. CVD Growth of Atomic Layer Heterostructures

The fabrication of desired atomic layer heterostructures is one of the most important challenges in current research on two-dimensional materials.[142)] For example, the use of hBN as a substrate allows us to access the intrinsic transport properties of graphene.[21)] Until now, research on atomic layer heterostructures has mainly focused on two different types of structures, namely, vertically stacked atomic layers, the so-called van der Walls heterostructures,[142)] and in-plane (lateral) heterostructures. Actual forms of these structures have been realized over the last several years, and attract much attention. For the controlled fabrication of these systems, vapor-phase growth techniques including CVD definitely play an important role. In the following section, we briefly review current topics and challenges in growth studies of heterostructures based on atomic layers.

In initial studies, van der Waals heterostructures have been primarily prepared by mechanical exfoliation and multiple transfers of atomic layers of materials such as graphene, boron nitride, and transition metal dichalcogenides (TMDCs).[21,143–145)] Although the exfoliation and transfer processes are basically simple and have been improved to produce clean heterostructures,[143,146)] several challenges still exist. For example, during the transfer, the samples may accidentally have ripples, impurities, lattice strain, and cracks. These factors could deteriorate interlayer coupling and charge transport properties. Additional heat treatment is sometimes necessary to remove impurities such as water for the improvement of interlayer coupling and flatness.[147)] Furthermore, the size of exfoliated samples is severely limited for device applications. To overcome this difficulty, many research groups have tried to develop direct growth techniques for producing clean and large-area heterostructures. One of the most important challenges is the direct growth of high-quality graphene on hBN (and hBN growth on graphene). To develop wafer-scale, high-performance graphene-based devices, the direct growth has been tried by various vapor phase growth techniques including CVD.[22,148,149)] In particular, a plasma-assisted deposition method enables the epitaxial growth of graphene single crystals on hBN with a fixed stacking orientation (Fig. 8).[22)] There have been, however, no reports on high carrier mobilities of CVD graphene directly grown hBN. Further improvement and preferably breakthroughs are essential for the direct growth of graphene and hBN systems.

Similar vertical heterostructures are also realized for the combination of graphene (or hBN) and TMDCs, and two different types of TMDCs. In the former case, TMDCs are normally grown on graphene (graphite) and hBN,[23–25,128,141,150–154)] because the growth of TMDC does not require catalytic substrates and can be induced on various types of substrates with high chemical and thermal stabilities in the presence of sulfur and transition metals. In this regard, graphene (graphite) and hBN are ideal substrates because of their atomically flat surfaces, inert surface properties, and exceptional chemical and thermal stabilities (Fig. 9). In particular, exfoliated surfaces are very clean and are used to grow high-quality TMDCs, as confirmed by the uniform optical spectra of TMDCs (Fig. 10).[24,25)] The preparation of such high-quality samples will enable further investigation of the intrinsic properties of atomic layer TMDCs. This approach would, therefore, be useful for the growth of unexplored two-dimensional materials as well as of TMDCs.

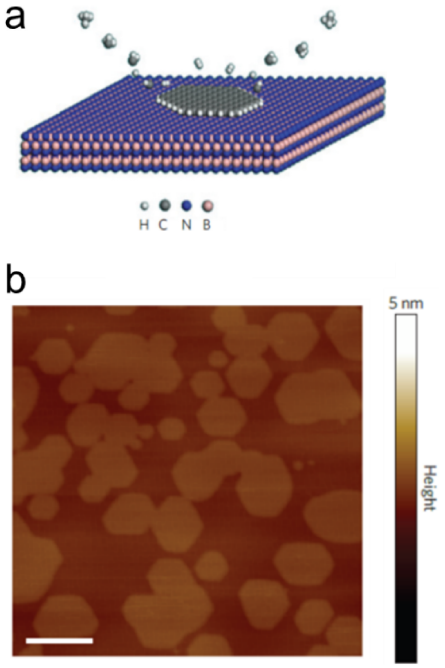

Fig. 8. (Color online) (a) Schematic illustration of the growth mechanism. (b) Atomic force microscopy image of as-grown graphene showing aligned hexagonal grains. The scale bar is 200 nm. Reproduced from Ref. 22.

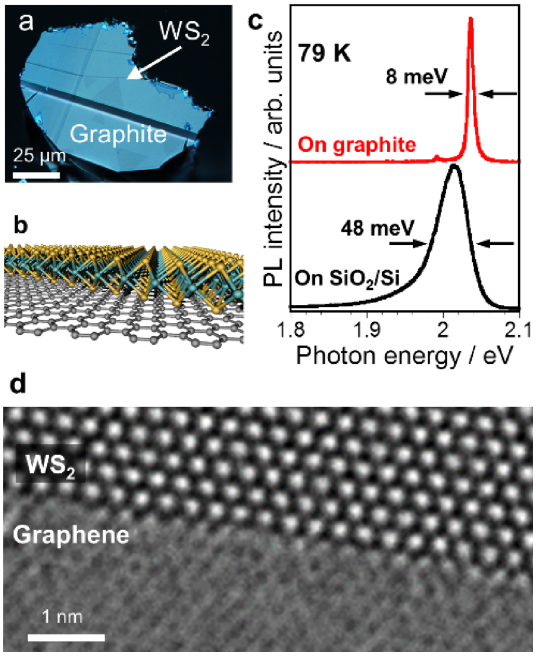

Fig. 10. (Color online) (a) Optical microscopy image and (b) schematic illustration of WS_2 monolayers grown on graphite (graphene). (c) Photoluminescence spectra of WS_2 monolayers grown on graphite and SiO_2/Si substrates measured at 79 K. (d) High-resolution TEM image of few-layer WS_2 grown on graphene. Reproduced from Ref. 25.

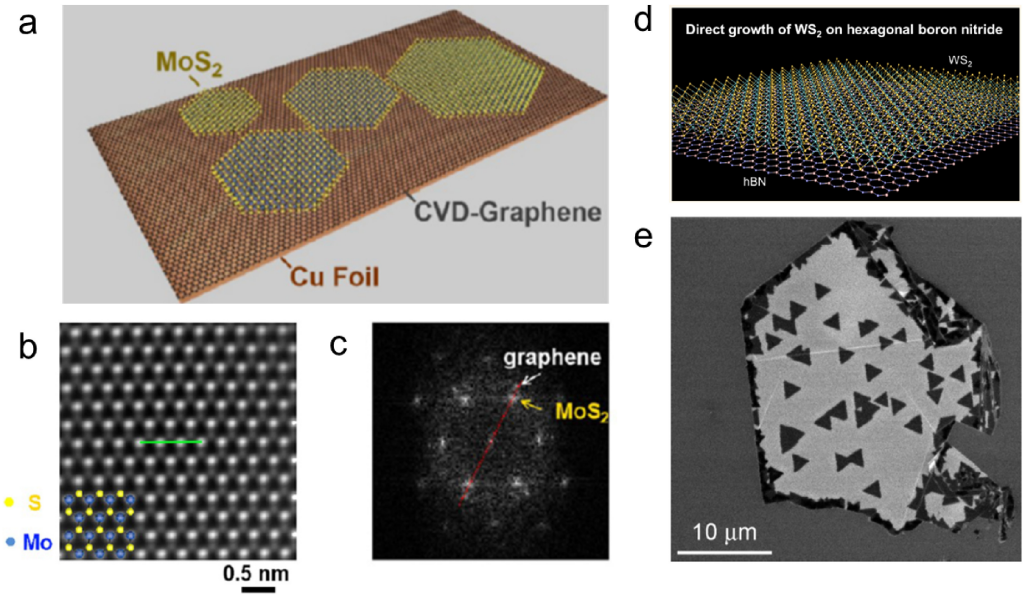

Fig. 9. (Color online) (a) Schematic illustration of atomically thin MoS_2 grains grown on graphene. (b) Fast Fourier transform (FFT)-filtered image of high-resolution scanning transmission electron microscopy (STEM) imaging of the monolayer MoS_2 film supported on the graphene membrane. (c) FFT pattern from the STEM image of the monolayer MoS_2 film supported on the graphene membrane. Reproduced from Ref. 23. (d) Schematic illustration and (e) SEM image of monolayer WS_2 grown on hBN. Reproduced from Ref. 24.

In the latter case, TMDC-based vertical WS_2/MoS_2 bilayers have recently been formed through CVD processes (Fig. 11).[155] In this case, Mo atoms contribute to crystal growth at an earlier stage than W atoms, resulting in the self-assembly of TMDC-based heterostructures even in the case of a single-step growth process. The same approach has also been applied to the formation of lateral heterostructures based on TMDCs, as described below.

In addition to such vertical heterostructures, recent progresses in growth techniques such as CVD and physical vapor transport have allowed for the synthesis of lateral heterostructures based on monolayer graphene/boron nitrides[156–163] and two different types of monolayer TMDCs.[155,164–166] One of the most interesting aspects is that lateral heterostructures have one-dimensional interfaces, which have been theoretically predicted to exhibit unique electric and magnetic properties such as half-metal and spin polarization.[167–169] Recently, TMDC-based lateral heterostructures have attracted much attention owing to their semiconducting properties, which are essential for the

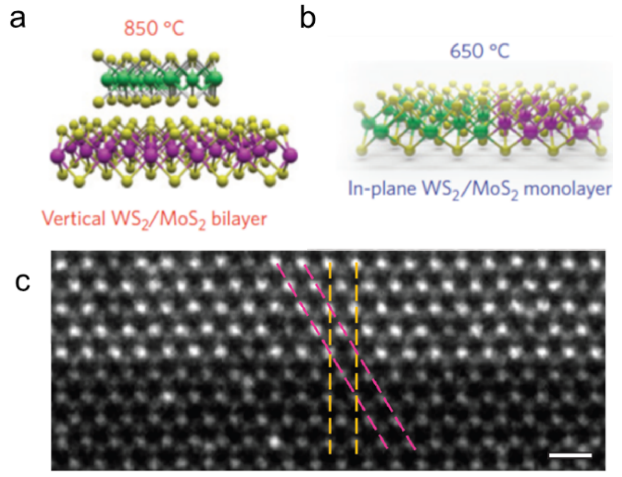

Fig. 11. (Color online) Schematic illustrations of (a) the vertically stacked WS_2/MoS_2 heterostructures synthesized at 850 °C and (b) the WS_2/MoS_2 in-plane heterojunctions grown at 650 °C. (c) Atomic resolution *Z*-contrast STEM images of the in-plane interface between WS_2 and MoS_2 domain. The scale bar is 0.5 nm. Reproduced from Ref. 155.

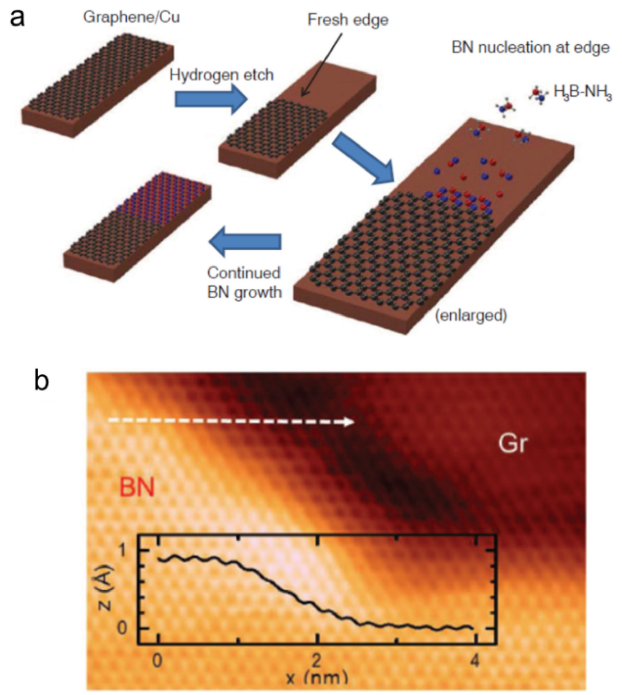

Fig. 12. (Color online) (a) Schematic illustration of epitaxial growth of hBN at graphene edges. Black, blue, red, and small gray spheres indicate C, N, B, and H atoms, respectively. (b) Scanning tunneling microscopy image at a graphene–BN boundary ($7.5 \times 5\,nm^2$; sample bias: 0.5 V). (Inset) Height profile along the white dashed arrow across the boundary. Reproduced from Ref. 160.

realization of novel functional electronics and optoelectronics such as chiral light-emitting devices.

Basically, lateral heterostructures can be prepared through the two-step growth process. For graphene/hBN lateral heterostructures,[156–163] individual grains of monolayer graphene are usually synthesized from carbon sources such as methane, and hBN monolayers are, then, grown from ammonia borane (or borazine) on the same substrates, as illustrated in Fig. 12. When the hBN growth is initiated preferentially at the edge of graphene grains, the crystallographic orientation of hBN can be determined by the structure of graphene edges. This edge-initiated growth can be regarded as one-dimensional heteroepitaxy, where graphene edges act as an epitaxial substrate for the hBN growth. It is noted that a similar process can produce a unique monolayer alloy based on boron, carbon, and nitrogen atoms.[170,171] For TMDC-based lateral heterostructures,[155,164–166] various combinations are adopted mainly for semiconducting Mo- and W-based TMDCs such as MoS_2, $MoSe_2$, WS_2, and WSe_2 (Fig. 11). More recently, similar lateral heterostructures have been demonstrated for monolayer $Mo_{1-x}W_xS_2$ TMDC alloys, which have composition-dependent tunable bandgaps.[172] Because of the many compositional variations of TMDC series, more studies will be expected for the growth of various TMDC-based heterostructures with novel functionalities.

6. Summary

In this review article, we have focused on CVD growth of atomic layers and atomic-layer heterostructures. After the discovery of graphene, growth technique of atomic layers has greatly advanced and past 10-years research has proven that there is a very bright future in science and application of atomic layers. The wide variety of atomic layers, graphene, hBN, TMDCs and heterostructures, have been emerging from CVD growth, and these CVD-grown large-area structure-defined 2-dimensional materials have been providing a platform to test basic questions in 2-dimensional systems. In addition, unique characteristics of atomic layers, such as ultra-thin structure, high carrier mobility and high-performance FET action, have clearly demonstrated the enormous possibility in future applications. Significant research efforts, by physicists, chemists, materials scientists, have been devoted to growth and characterization of atomic layers, which leads to basic understanding of the growth and properties of atomic layers. These basic understandings on the fundamentals of atomic layers will make quantum jumps toward a rich array of future science and technologies.

1) J. W. May, Surf. Sci. **17**, 267 (1969).
2) R. S. Ruoff, MRS Bull. **37** [12], 1314 (2012).
3) K. S. Novoselov, A. K. Geim, S. V. Morozov, D. Jiang, Y. Zhang, S. V. Dubonos, I. V. Grigorieva, and A. A. Firsov, Science **306**, 666 (2004).
4) K. S. Novoselov, A. K. Geim, S. V. Morozov, D. Jiang, M. I. Katsnelson, I. V. Grigorieva, S. V. Dubonos, and A. A. Firsov, Nature **438**, 197 (2005).
5) A. K. Geim and K. S. Novoselov, Nat. Mater. **6**, 183 (2007).
6) A. H. Castro Neto, F. Guinea, N. M. R. Peres, K. S. Novoselov, and A. K. Geim, Rev. Mod. Phys. **81**, 109 (2009).
7) C. Berger, Z. M. Song, T. B. Li, X. B. Li, A. Y. Ogbazghi, R. Feng, Z. T. Dai, A. N. Marchenkov, E. H. Conrad, P. N. First, and W. A. de Heer, J. Phys. Chem. B **108**, 19912 (2004).
8) Y. B. Zhang, Y. W. Tan, H. L. Stormer, and P. Kim, Nature **438**, 201 (2005).
9) S. Z. Butler, S. M. Hollen, L. Y. Cao, Y. Cui, J. A. Gupta, H. R. Gutierrez, T. F. Heinz, S. S. Hong, J. X. Huang, A. F. Ismach, E. Johnston-Halperin, M. Kuno, V. V. Plashnitsa, R. D. Robinson, R. S. Ruoff, S. Salahuddin, J. Shan, L. Shi, M. G. Spencer, M. Terrones, W. Windl, and J. E. Goldberger, ACS Nano **7**, 2898 (2013).
10) K. F. Mak, C. Lee, J. Hone, J. Shan, and T. F. Heinz, Phys. Rev. Lett. **105**, 136805 (2010).
11) Y. Lin and J. W. Connell, Nanoscale **4**, 6908 (2012).

12) Q. H. Wang, K. Kalantar-Zadeh, A. Kis, J. N. Coleman, and M. S. Strano, Nat. Nanotechnol. **7**, 699 (2012).
13) R. F. Frindt, J. Appl. Phys. **37**, 1928 (1966).
14) K. S. Novoselov, D. Jiang, F. Schedin, T. J. Booth, V. V. Khotkevich, S. V. Morozov, and A. K. Geim, Proc. Natl. Acad. Sci. U.S.A. **102**, 10451 (2005).
15) R. V. Gorbachev, I. Riaz, R. R. Nair, R. Jalil, L. Britnell, B. D. Belle, E. W. Hill, K. S. Novoselov, K. Watanabe, T. Taniguchi, A. K. Geim, and P. Blake, Small **7**, 465 (2011).
16) D. Yang, S. J. Sandoval, W. M. R. Divigalpitiya, J. C. Irwin, and R. F. Frindt, Phys. Rev. B **43**, 12053 (1991).
17) K. I. Bolotin, F. Ghahari, M. D. Shulman, H. L. Stormer, and P. Kim, Nature **462**, 196 (2009).
18) B. Radisavljevic, A. Radenovic, J. Brivio, V. Giacometti, and A. Kis, Nat. Nanotechnol. **6**, 147 (2011).
19) K. F. Mak, K. L. He, J. Shan, and T. F. Heinz, Nat. Nanotechnol. **7**, 494 (2012).
20) D. Xiao, G. B. Liu, W. X. Feng, X. D. Xu, and W. Yao, Phys. Rev. Lett. **108**, 196802 (2012).
21) C. R. Dean, A. F. Young, I. Meric, C. Lee, L. Wang, S. Sorgenfrei, K. Watanabe, T. Taniguchi, P. Kim, K. L. Shepard, and J. Hone, Nat. Nanotechnol. **5**, 722 (2010).
22) W. Yang, G. Chen, Z. Shi, C. C. Liu, L. Zhang, G. Xie, M. Cheng, D. Wang, R. Yang, D. Shi, K. Watanabe, T. Taniguchi, Y. Yao, Y. Zhang, and G. Zhang, Nat. Mater. **12**, 792 (2013).
23) Y. M. Shi, W. Zhou, A. Y. Lu, W. J. Fang, Y. H. Lee, A. L. Hsu, S. M. Kim, K. K. Kim, H. Y. Yang, L. J. Li, J. C. Idrobo, and J. Kong, Nano Lett. **12**, 2784 (2012).
24) M. Okada, T. Sawazaki, K. Watanabe, T. Taniguch, H. Hibino, H. Shinohara, and R. Kitaura, ACS Nano **8**, 8273 (2014).
25) Y. Kobayashi, S. Sasaki, S. Mori, H. Hibino, Z. Liu, K. Watanabe, T. Taniguchi, K. Suenaga, Y. Maniwa, and Y. Miyata, ACS Nano **9**, 4056 (2015).
26) H. P. Boehm, R. Setton, and E. Stumpp, Carbon **24**, 241 (1986).
27) A. K. Geim and A. H. MacDonald, Phys. Today **60** [8], 35 (2007).
28) Editorial, Nat. Nanotechnol. **5**, 755 (2010).
29) C. Lee, X. D. Wei, J. W. Kysar, and J. Hone, Science **321**, 385 (2008).
30) S. Stankovich, D. A. Dikin, G. H. B. Dommett, K. M. Kohlhaas, E. J. Zimney, E. A. Stach, R. D. Piner, S. T. Nguyen, and R. S. Ruoff, Nature **442**, 282 (2006).
31) A. A. Balandin, S. Ghosh, W. Z. Bao, I. Calizo, D. Teweldebrhan, F. Miao, and C. N. Lau, Nano Lett. **8**, 902 (2008).
32) M. D. Stoller, S. J. Park, Y. W. Zhu, J. H. An, and R. S. Ruoff, Nano Lett. **8**, 3498 (2008).
33) F. Schedin, A. K. Geim, S. V. Morozov, E. W. Hill, P. Blake, M. I. Katsnelson, and K. S. Novoselov, Nat. Mater. **6**, 652 (2007).
34) F. Bonaccorso, Z. Sun, T. Hasan, and A. C. Ferrari, Nat. Photonics **4**, 611 (2010).
35) S. Stankovich, D. A. Dikin, R. D. Piner, K. A. Kohlhaas, A. Kleinhammes, Y. Jia, Y. Wu, S. T. Nguyen, and R. S. Ruoff, Carbon **45**, 1558 (2007).
36) S. Park and R. S. Ruoff, Nat. Nanotechnol. **4**, 217 (2009).
37) K. S. Kim, Y. Zhao, H. Jang, S. Y. Lee, J. M. Kim, K. S. Kim, J. H. Ahn, P. Kim, J. Y. Choi, and B. H. Hong, Nature **457**, 706 (2009).
38) A. Reina, X. T. Jia, J. Ho, D. Nezich, H. B. Son, V. Bulovic, M. S. Dresselhaus, and J. Kong, Nano Lett. **9**, 30 (2009).
39) In "Web of Science", searching "synthesis graphene" OR "production graphene" OR "growth graphene" in "title" finds 4,036 records, within which 3,176 records have "chemical vapor deposition" in its "topic".
40) J. Kong, A. M. Cassell, and H. J. Dai, Chem. Phys. Lett. **292**, 567 (1998).
41) B. C. Banerjee, P. L. Walker, and T. J. Hirt, Nature **192**, 450 (1961).
42) J. C. Shelton, H. R. Patil, and J. M. Blakely, Surf. Sci. **43**, 493 (1974).
43) M. Eizenberg and J. M. Blakely, Surf. Sci. **82**, 228 (1979).
44) L. Zhao, K. T. Rim, H. Zhou, R. He, T. F. Heinz, A. Pinczuk, G. W. Flynn, and A. N. Pasupathy, Solid State Commun. **151**, 509 (2011).
45) J. M. Wofford, S. Nie, K. F. McCarty, N. C. Bartelt, and O. D. Dubon, Nano Lett. **10**, 4890 (2010).
46) P. R. Somani, S. P. Somani, and M. Umeno, Chem. Phys. Lett. **430**, 56 (2006).
47) A. N. Obraztsov, E. A. Obraztsova, A. V. Tyurnina, and A. A. Zolotukhin, Carbon **45**, 2017 (2007).
48) Q. K. Yu, J. Lian, S. Siriponglert, H. Li, Y. P. Chen, and S. S. Pei, Appl. Phys. Lett. **93**, 113103 (2008).
49) S. J. Chae, F. Gunes, K. K. Kim, E. S. Kim, G. H. Han, S. M. Kim, H. J. Shin, S. M. Yoon, J. Y. Choi, M. H. Park, C. W. Yang, D. Pribat, and Y. H. Lee, Adv. Mater. **21**, 2328 (2009).
50) X. S. Li, W. W. Cai, L. Colombo, and R. S. Ruoff, Nano Lett. **9**, 4268 (2009).
51) R. S. Weatherup, B. Dlubak, and S. Hofmann, ACS Nano **6**, 9996 (2012).
52) R. Addou, A. Dahal, P. Sutter, and M. Batzill, Appl. Phys. Lett. **100**, 021601 (2012).
53) E. Sutter, P. Albrecht, and P. Sutter, Appl. Phys. Lett. **95**, 133109 (2009).
54) P. W. Sutter, P. M. Albrecht, and E. A. Sutter, Appl. Phys. Lett. **97**, 213101 (2010).
55) D. Eom, D. Prezzi, K. T. Rim, H. Zhou, M. Lefenfeld, S. Xiao, C. Nuckolls, M. S. Hybertsen, T. F. Heinz, and G. W. Flynn, Nano Lett. **9**, 2844 (2009).
56) S. Y. Kwon, C. V. Ciobanu, V. Petrova, V. B. Shenoy, J. Bareno, V. Gambin, I. Petrov, and S. Kodambaka, Nano Lett. **9**, 3985 (2009).
57) B. Wang, M. Caffio, C. Bromley, H. Fruchtl, and R. Schaub, ACS Nano **4**, 5773 (2010).
58) T. Oznuluer, E. Pince, E. O. Polat, O. Balci, O. Salihoglu, and C. Kocabas, Appl. Phys. Lett. **98**, 183101 (2011).
59) P. Sutter, J. T. Sadowski, and E. Sutter, Phys. Rev. B **80**, 245411 (2009).
60) A. T. N'Diaye, J. Coraux, T. N. Plasa, C. Busse, and T. Michely, New J. Phys. **10**, 043033 (2008).
61) E. Miniussi, M. Pozzo, A. Baraldi, E. Vesselli, R. R. Zhan, G. Comelli, T. O. Mentes, M. A. Nino, A. Locatelli, S. Lizzit, and D. Alfe, Phys. Rev. Lett. **106**, 216101 (2011).
62) Y. Pan, H. G. Zhang, D. X. Shi, J. T. Sun, S. X. Du, F. Liu, and H. J. Gao, Adv. Mater. **21**, 2777 (2009).
63) Y. Que, W. Xiao, X. Fei, H. Chen, L. Huang, S. X. Du, and H.-J. Gao, Appl. Phys. Lett. **104**, 093110 (2014).
64) S. Marchini, S. Gunther, and J. Wintterlin, Phys. Rev. B **76**, 075429 (2007).
65) D. Martoccia, P. R. Willmott, T. Brugger, M. Björck, S. Günther, C. M. Schlepütz, A. Cervellino, S. A. Pauli, B. D. Patterson, S. Marchini, J. Wintterlin, W. Moritz, and T. Greber, Phys. Rev. Lett. **101**, 126102 (2008).
66) D. E. Jiang, M. H. Du, and S. Dai, J. Chem. Phys. **130**, 074705 (2009).
67) D. Stradi, S. Barja, C. Diaz, M. Garnica, B. Borca, J. J. Hinarejos, D. Sanchez-Portal, M. Alcami, A. Arnau, A. L. V. de Parga, R. Miranda, and F. Martin, Phys. Rev. Lett. **106**, 186102 (2011).
68) M. Gao, Y. Pan, L. Huang, H. Hu, L. Z. Zhang, H. M. Guo, S. X. Du, and H. J. Gao, Appl. Phys. Lett. **98**, 033101 (2011).
69) T. Gao, S. B. Xie, Y. B. Gao, M. X. Liu, Y. B. Chen, Y. F. Zhang, and Z. F. Liu, ACS Nano **5**, 9194 (2011).
70) L. B. Gao, W. C. Ren, H. L. Xu, L. Jin, Z. X. Wang, T. Ma, L. P. Ma, Z. Y. Zhang, Q. Fu, L. M. Peng, X. H. Bao, and H. M. Cheng, Nat. Commun. **3**, 699 (2012).
71) B. Y. Dai, L. Fu, Z. Y. Zou, M. Wang, H. T. Xu, S. Wang, and Z. F. Liu, Nat. Commun. **2**, 522 (2011).
72) X. S. Li, W. W. Cai, J. H. An, S. Kim, J. Nah, D. X. Yang, R. Piner, A. Velamakanni, I. Jung, E. Tutuc, S. K. Banerjee, L. Colombo, and R. S. Ruoff, Science **324**, 1312 (2009).
73) L. Liu and S. S. Fan, J. Am. Chem. Soc. **123**, 11502 (2001).
74) F. Simon, C. Kramberger, R. Pfeiffer, H. Kuzmany, V. Zolyomi, J. Kurti, P. M. Singer, and H. Alloul, Phys. Rev. Lett. **95**, 017401 (2005).
75) R. Xiang, B. Hou, E. Einarsson, P. Zhao, S. Harish, K. Morimoto, Y. Miyauchi, S. Chiashi, Z. K. Tang, and S. Maruyama, ACS Nano **7**, 3095 (2013).
76) S. S. Chen, H. X. Ji, H. Chou, Q. Y. Li, H. Y. Li, J. W. Suk, R. Piner, L. Liao, W. W. Cai, and R. S. Ruoff, Adv. Mater. **25**, 2062 (2013).
77) Y. F. Hao, M. S. Bharathi, L. Wang, Y. Y. Liu, H. Chen, S. Nie, X. H. Wang, H. Chou, C. Tan, B. Fallahazad, H. Ramanarayan, C. W. Magnuson, E. Tutuc, B. I. Yakobson, K. F. McCarty, Y. W. Zhang, P. Kim, J. Hone, L. Colombo, and R. S. Ruoff, Science **342**, 720 (2013).
78) H. Zhou, W. J. Yu, L. Liu, R. Cheng, Y. Chen, X. Huang, Y. Liu, Y. Wang, Y. Huang, and X. Duan, Nat. Commun. **4**, 2096 (2013).
79) Q. Yu, L. A. Jauregui, W. Wu, R. Colby, J. Tian, Z. Su, H. Cao, Z. Liu, D. Pandey, D. Wei, T. F. Chung, P. Peng, N. P. Guisinger, E. A.

Stach, J. Bao, S.-S. Pei, and Y. P. Chen, Nat. Mater. **10**, 443 (2011).
80) S. Bae, H. Kim, Y. Lee, X. F. Xu, J. S. Park, Y. Zheng, J. Balakrishnan, T. Lei, H. R. Kim, Y. I. Song, Y. J. Kim, K. S. Kim, B. Ozyilmaz, J. H. Ahn, B. H. Hong, and S. Iijima, Nat. Nanotechnol. **5**, 574 (2010).
81) L. Brown, E. B. Lochocki, J. Avila, C. J. Kim, Y. Ogawa, R. W. Havener, D. K. Kim, E. J. Monkman, D. E. Shai, H. F. I. Wei, M. P. Levendorf, M. Asensio, K. M. Shen, and J. Park, Nano Lett. **14**, 5706 (2014).
82) V. L. Nguyen, B. G. Shin, D. L. Duong, S. T. Kim, D. Perello, Y. J. Lim, Q. H. Yuan, F. Ding, H. Y. Jeong, H. S. Shin, S. M. Lee, S. H. Chae, Q. A. Vu, S. H. Lee, and Y. H. Lee, Adv. Mater. **27**, 1376 (2015).
83) O. V. Yazyev and Y. P. Chen, Nat. Nanotechnol. **9**, 755 (2014).
84) X. S. Li, C. W. Magnuson, A. Venugopal, R. M. Tromp, J. B. Hannon, E. M. Vogel, L. Colombo, and R. S. Ruoff, J. Am. Chem. Soc. **133**, 2816 (2011).
85) Z. Yan, J. Lin, Z. W. Peng, Z. Z. Sun, Y. Zhu, L. Li, C. S. Xiang, E. L. Samuel, C. Kittrell, and J. M. Tour, ACS Nano **6**, 9110 (2012).
86) A. Mohsin, L. Liu, P. Z. Liu, W. Deng, I. N. Ivanov, G. L. Li, O. E. Dyck, G. Duscher, J. R. Dunlap, K. Xiao, and G. Gu, ACS Nano **7**, 8924 (2013).
87) L. Gan and Z. T. Luo, ACS Nano **7**, 9480 (2013).
88) J. H. Hafner, M. J. Bronikowski, B. R. Azamian, P. Nikolaev, A. G. Rinzler, D. T. Colbert, K. A. Smith, and R. E. Smalley, Chem. Phys. Lett. **296**, 195 (1998).
89) R. Xiang, Z. Yang, Q. Zhang, G. H. Luo, W. Z. Qian, F. Wei, M. Kadowaki, E. Einarsson, and S. Maruyama, J. Phys. Chem. C **112**, 4892 (2008).
90) J. H. Lee, E. K. Lee, W. J. Joo, Y. Jang, B. S. Kim, J. Y. Lim, S. H. Choi, S. J. Ahn, J. R. Ahn, M. H. Park, C. W. Yang, B. L. Choi, S. W. Hwang, and D. Whang, Science **344**, 286 (2014).
91) L. Gao, J. R. Guest, and N. P. Guisinger, Nano Lett. **10**, 3512 (2010).
92) Y. Ogawa, B. S. Hu, C. M. Orofeo, M. Tsuji, K. Ikeda, S. Mizuno, H. Hibino, and H. Ago, J. Phys. Chem. Lett. **3**, 219 (2012).
93) G. Nandamuri, S. Roumimov, and R. Solanki, Nanotechnology **21**, 145604 (2010).
94) Y. G. Yao, Z. Li, Z. Y. Lin, K. S. Moon, J. Agar, and C. P. Wong, J. Phys. Chem. C **115**, 5232 (2011).
95) Z. C. Li, P. Wu, C. X. Wang, X. D. Fan, W. H. Zhang, X. F. Zhai, C. G. Zeng, Z. Y. Li, J. L. Yang, and J. G. Hou, ACS Nano **5**, 3385 (2011).
96) J.-H. Choi, Z. Li, P. Cui, X. Fan, H. Zhang, C. Zeng, and Z. Zhang, Sci. Rep. **3**, 1925 (2013).
97) Z. Z. Sun, Z. Yan, J. Yao, E. Beitler, Y. Zhu, and J. M. Tour, Nature **468**, 549 (2010).
98) A. Delamoreanu, C. Rabot, C. Vallee, and A. Zenasni, Carbon **66**, 48 (2014).
99) G. D. Ruan, Z. Z. Sun, Z. W. Peng, and J. M. Tour, ACS Nano **5**, 7601 (2011).
100) S. Maruyama, R. Kojima, Y. Miyauchi, S. Chiashi, and M. Kohno, Chem. Phys. Lett. **360**, 229 (2002).
101) Y. Miyata, K. Kamon, K. Ohashi, R. Kitaura, M. Yoshimura, and H. Shinohara, Appl. Phys. Lett. **96**, 263105 (2010).
102) A. Guermoune, T. Chari, F. Popescu, S. S. Sabri, J. Guillemette, H. S. Skulason, T. Szkopek, and M. Siaj, Carbon **49**, 4204 (2011).
103) P. Zhao, B. Hou, X. Chen, S. Kim, S. Chiashi, E. Einarsson, and S. Maruyama, Nanoscale **5**, 6530 (2013).
104) X. Chen, P. Zhao, R. Xiang, S. Kim, J. Cha, S. Chiashi, and S. Maruyama, Carbon **94**, 810 (2015).
105) P. Zhao, S. Kim, X. Chen, E. Einarsson, M. Wang, Y. N. Song, H. T. Wang, S. Chiashi, R. Xiang, and S. Maruyama, ACS Nano **8**, 11631 (2014).
106) Q. Y. Li, H. Chou, J. H. Zhong, J. Y. Liu, A. Dolocan, J. Y. Zhang, Y. H. Zhou, R. S. Ruoff, S. S. Chen, and W. W. Cai, Nano Lett. **13**, 486 (2013).
107) W. Fang, A. L. Hsu, R. Caudillo, Y. Song, A. G. Birdwell, E. Zakar, M. Kalbac, M. Dubey, T. Palacios, M. S. Dresselhaus, P. T. Araujo, and J. Kong, Nano Lett. **13**, 1541 (2013).
108) C. M. Orofeo, S. Suzuki, H. Kageshima, and H. Hibino, Nano Res. **6**, 335 (2013).
109) L. Song, L. Ci, H. Lu, P. B. Sorokin, C. Jin, J. Ni, A. G. Kvashnin, D. G. Kvashnin, J. Lou, B. I. Yakobson, and P. M. Ajayan, Nano Lett. **10**, 3209 (2010).
110) K. K. Kim, A. Hsu, X. Jia, S. M. Kim, Y. Shi, M. Hofmann, D. Nezich, J. F. Rodriguez-Nieva, M. Dresselhaus, T. Palacios, and J. Kong, Nano Lett. **12**, 161 (2012).
111) K. H. Lee, H. J. Shin, J. Lee, I. Y. Lee, G. H. Kim, J. Y. Choi, and S. W. Kim, Nano Lett. **12**, 714 (2012).
112) G. Kim, A. R. Jang, H. Y. Jeong, Z. Lee, D. J. Kang, and H. S. Shin, Nano Lett. **13**, 1834 (2013).
113) K. K. Kim, A. Hsu, X. T. Jia, S. M. Kim, Y. M. Shi, M. Dresselhaus, T. Palacios, and J. Kong, ACS Nano **6**, 8583 (2012).
114) J. Lu, P. S. Yeo, Y. Zheng, H. Xu, C. K. Gan, M. B. Sullivan, A. H. Castro Neto, and K. P. Loh, J. Am. Chem. Soc. **135**, 2368 (2013).
115) Y. Shi, C. Hamsen, X. Jia, K. K. Kim, A. Reina, M. Hofmann, A. L. Hsu, K. Zhang, H. Li, Z. Y. Juang, M. S. Dresselhaus, L. J. Li, and J. Kong, Nano Lett. **10**, 4134 (2010).
116) S. Joshi, D. Ecija, R. Koitz, M. Iannuzzi, A. P. Seitsonen, J. Hutter, H. Sachdev, S. Vijayaraghavan, F. Bischoff, K. Seufert, J. V. Barth, and W. Auwarter, Nano Lett. **12**, 5821 (2012).
117) A. Ismach, H. Chou, D. A. Ferrer, Y. P. Wu, S. McDonnell, H. C. Floresca, A. Covacevich, C. Pope, R. Piner, M. J. Kim, R. M. Wallace, L. Colombo, and R. S. Ruoff, ACS Nano **6**, 6378 (2012).
118) T. Taniguchi and K. Watanabe, J. Cryst. Growth **303**, 525 (2007).
119) Y. Kubota, K. Watanabe, O. Tsuda, and T. Taniguchi, Science **317**, 932 (2007).
120) A. L. Gibb, N. Alem, J.-H. Chen, K. J. Erickson, J. Ciston, A. Gautam, M. Linck, and A. Zettl, J. Am. Chem. Soc. **135**, 6758 (2013).
121) K. F. Mak, K. He, J. Shan, and T. F. Heinz, Nat. Nanotechnol. **7**, 494 (2012).
122) H. Zeng, J. Dai, W. Yao, D. Xiao, and X. Cui, Nat. Nanotechnol. **7**, 490 (2012).
123) K. F. Mak, K. L. McGill, J. Park, and P. L. McEuen, Science **344**, 1489 (2014).
124) X. D. Xu, W. Yao, D. Xiao, and T. F. Heinz, Nat. Phys. **10**, 343 (2014).
125) Y. H. Lee, X. Q. Zhang, W. J. Zhang, M. T. Chang, C. T. Lin, K. D. Chang, Y. C. Yu, J. T. W. Wang, C. S. Chang, L. J. Li, and T. W. Lin, Adv. Mater. **24**, 2320 (2012).
126) A. M. van der Zande, P. Y. Huang, D. A. Chenet, T. C. Berkelbach, Y. You, G. H. Lee, T. F. Heinz, D. R. Reichman, D. A. Muller, and J. C. Hone, Nat. Mater. **12**, 554 (2013).
127) S. S. Wang, Y. M. Rong, Y. Fan, M. Pacios, H. Bhaskaran, K. He, and J. H. Warner, Chem. Mater. **26**, 6371 (2014).
128) X. Ling, Y. H. Lee, Y. X. Lin, W. J. Fang, L. L. Yu, M. S. Dresselhaus, and J. Kong, Nano Lett. **14**, 464 (2014).
129) Y. H. Chang, W. Zhang, Y. Zhu, Y. Han, J. Pu, J. K. Chang, W. T. Hsu, J. K. Huang, C. L. Hsu, M. H. Chiu, T. Takenobu, H. Li, C. I. Wu, W. H. Chang, A. T. S. Wee, and L. J. Li, ACS Nano **8**, 8582 (2014).
130) G. W. Shim, K. Yoo, S. B. Seo, J. Shin, D. Y. Jung, I. S. Kang, C. W. Ahn, B. J. Cho, and S. Y. Choi, ACS Nano **8**, 6655 (2014).
131) K. K. Liu, W. J. Zhang, Y. H. Lee, Y. C. Lin, M. T. Chang, C. Su, C. S. Chang, H. Li, Y. M. Shi, H. Zhang, C. S. Lai, and L. J. Li, Nano Lett. **12**, 1538 (2012).
132) Q. Q. Ji, Y. F. Zhang, T. Gao, Y. Zhang, D. L. Ma, M. X. Liu, Y. B. Chen, X. F. Qiao, P. H. Tan, M. Kan, J. Feng, Q. Sun, and Z. F. Liu, Nano Lett. **13**, 3870 (2013).
133) J. K. Huang, J. Pu, C. L. Hsu, M. H. Chiu, Z. Y. Juang, Y. H. Chang, W. H. Chang, Y. Iwasa, T. Takenobu, and L. J. Li, ACS Nano **8**, 923 (2014).
134) Y. Zhang, Y. F. Zhang, Q. Q. Ji, J. Ju, H. T. Yuan, J. P. Shi, T. Gao, D. L. Ma, M. X. Liu, Y. B. Chen, X. J. Song, H. Y. Hwang, Y. Cui, and Z. F. Liu, ACS Nano **7**, 8963 (2013).
135) A. L. Elías, N. Perea-López, A. Castro-Beltrán, A. Berkdemir, R. Lv, S. Feng, A. D. Long, T. Hayashi, Y. A. Kim, M. Endo, H. R. Gutiérrez, N. R. Pradhan, L. Balicas, T. E. Mallouk, F. López-Urías, H. Terrones, and M. Terrones, ACS Nano **7**, 5235 (2013).
136) Y. M. Rong, Y. Fan, A. L. Koh, A. W. Robertson, K. He, S. S. Wang, H. J. Tan, R. Sinclair, and J. H. Warner, Nanoscale **6**, 12096 (2014).
137) H. R. Gutiérrez, N. Perea-López, A. L. Elías, A. Berkdemir, B. Wang, R. Lv, F. López-Urías, V. H. Crespi, H. Terrones, and M. Terrones, Nano Lett. **13**, 3447 (2013).
138) H. Yamamoto, K. Yoshii, K. Saiki, and A. Koma, J. Vac. Sci. Technol. A **12**, 125 (1994).

139) F. S. Ohuchi, B. A. Parkinson, K. Ueno, and A. Koma, J. Appl. Phys. **68**, 2168 (1990).
140) R. Y. Yue, A. T. Barton, H. Zhu, A. Azcatl, L. F. Pena, J. Wang, X. Peng, N. Lu, L. X. Cheng, R. Addou, S. McDonnell, L. Colombo, J. W. P. Hsu, J. Kim, M. J. Kim, R. M. Wallace, and C. L. Hinkle, ACS Nano **9**, 474 (2015).
141) M. M. Ugeda, A. J. Bradley, S. F. Shi, F. H. da Jornada, Y. Zhang, D. Y. Qiu, W. Ruan, S. K. Mo, Z. Hussain, Z. X. Shen, F. Wang, S. G. Louie, and M. F. Crommie, Nat. Mater. **13**, 1091 (2014).
142) A. K. Geim and I. V. Grigorieva, Nature **499**, 419 (2013).
143) L. Wang, I. Meric, P. Y. Huang, Q. Gao, Y. Gao, H. Tran, T. Taniguchi, K. Watanabe, L. M. Campos, D. A. Muller, J. Guo, P. Kim, J. Hone, K. L. Shepard, and C. R. Dean, Science **342**, 614 (2013).
144) L. Britnell, R. V. Gorbachev, R. Jalil, B. D. Belle, F. Schedin, A. Mishchenko, T. Georgiou, M. I. Katsnelson, L. Eaves, S. V. Morozov, N. M. R. Peres, J. Leist, A. K. Geim, K. S. Novoselov, and L. A. Ponomarenko, Science **335**, 947 (2012).
145) L. Britnell, R. M. Ribeiro, A. Eckmann, R. Jalil, B. D. Belle, A. Mishchenko, Y. J. Kim, R. V. Gorbachev, T. Georgiou, S. V. Morozov, A. N. Grigorenko, A. K. Geim, C. Casiraghi, A. H. Castro Neto, and K. S. Novoselov, Science **340**, 1311 (2013).
146) C.-G. Andres, B. Michele, M. Rianda, S. Vibhor, J. Laurens, S. J. v. d. Z. Herre, and A. S. Gary, 2D Mater. **1**, 011002 (2014).
147) S. J. Haigh, A. Gholinia, R. Jalil, S. Romani, L. Britnell, D. C. Elias, K. S. Novoselov, L. A. Ponomarenko, A. K. Geim, and R. Gorbachev, Nat. Mater. **11**, 764 (2012).
148) Z. Liu, L. Song, S. Zhao, J. Huang, L. Ma, J. Zhang, J. Lou, and P. M. Ajayan, Nano Lett. **11**, 2032 (2011).
149) M. Wang, S. K. Jang, W. J. Jang, M. Kim, S. Y. Park, S. W. Kim, S. J. Kahng, J. Y. Choi, R. S. Ruoff, Y. J. Song, and S. Lee, Adv. Mater. **25**, 2746 (2013).
150) C. Zhang, A. Johnson, C.-L. Hsu, L.-J. Li, and C.-K. Shih, Nano Lett. **14**, 2443 (2014).
151) W. Ge, K. Kawahara, M. Tsuji, and H. Ago, Nanoscale **5**, 5773 (2013).
152) H. Ago, H. Endo, P. Solís-Fernández, R. Takizawa, Y. Ohta, Y. Fujita, K. Yamamoto, and M. Tsuji, ACS Appl. Mater. Interfaces **7**, 5265 (2015).
153) Y. C. Lin, C. Y. Chang, R. K. Ghosh, J. Li, H. Zhu, R. Addou, B. Diaconescu, T. Ohta, X. Peng, N. Lu, M. J. Kim, J. T. Robinson, R. M. Wallace, T. S. Mayer, S. Datta, L. J. Li, and J. A. Robinson, Nano Lett. **14**, 6936 (2014).
154) S. M. Eichfeld, L. Hossain, Y.-C. Lin, A. F. Piasecki, B. Kupp, A. G. Birdwell, R. A. Burke, N. Lu, X. Peng, J. Li, A. Azcatl, S. McDonnell, R. M. Wallace, M. J. Kim, T. S. Mayer, J. M. Redwing, and J. A. Robinson, ACS Nano **9**, 2080 (2015).
155) Y. Gong, J. Lin, X. Wang, G. Shi, S. Lei, Z. Lin, X. Zou, G. Ye, R. Vajtai, B. I. Yakobson, H. Terrones, M. Terrones, B. K. Tay, J. Lou, S. T. Pantelides, Z. Liu, W. Zhou, and P. M. Ajayan, Nat. Mater. **13**, 1135 (2014).
156) M. P. Levendorf, C.-J. Kim, L. Brown, P. Y. Huang, R. W. Havener, D. A. Muller, and J. Park, Nature **488**, 627 (2012).
157) P. Sutter, R. Cortes, J. Lahiri, and E. Sutter, Nano Lett. **12**, 4869 (2012).
158) Y. Miyata, E. Maeda, K. Kamon, R. Kitaura, Y. Sasaki, S. Suzuki, and H. Shinohara, Appl. Phys. Express **5**, 085102 (2012).
159) Z. Liu, L. Ma, G. Shi, W. Zhou, Y. Gong, S. Lei, X. Yang, J. Zhang, J. Yu, K. P. Hackenberg, A. Babakhani, J.-C. Idrobo, R. Vajtai, J. Lou, and P. M. Ajayan, Nat. Nanotechnol. **8**, 119 (2013).
160) L. Liu, J. Park, D. A. Siegel, K. F. McCarty, K. W. Clark, W. Deng, L. Basile, J. C. Idrobo, A. P. Li, and G. Gu, Science **343**, 163 (2014).
161) G. H. Han, J. A. Rodriguez-Manzo, C. W. Lee, N. J. Kybert, M. B. Lerner, Z. J. Qi, E. N. Dattoli, A. M. Rappe, M. Drndic, and A. T. C. Johnson, ACS Nano **7**, 10129 (2013).
162) R. W. Havener, C. J. Kim, L. Brown, J. W. Kevek, J. D. Sleppy, P. L. McEuen, and J. Park, Nano Lett. **13**, 3942 (2013).
163) Y. Gao, Y. Zhang, P. Chen, Y. Li, M. Liu, T. Gao, D. Ma, Y. Chen, Z. Cheng, X. Qiu, W. Duan, and Z. Liu, Nano Lett. **13**, 3439 (2013).
164) X. Duan, C. Wang, J. C. Shaw, R. Cheng, Y. Chen, H. Li, X. Wu, Y. Tang, Q. Zhang, A. Pan, J. Jiang, R. Yu, Y. Huang, and X. Duan, Nat. Nanotechnol. **9**, 1024 (2014).
165) C. Huang, S. Wu, A. M. Sanchez, J. J. Peters, R. Beanland, J. S. Ross, P. Rivera, W. Yao, D. H. Cobden, and X. Xu, Nat. Mater. **13**, 1096 (2014).
166) X. Q. Zhang, C. H. Lin, Y. W. Tseng, K. H. Huang, and Y. H. Lee, Nano Lett. **15**, 410 (2015).
167) S. Bhowmick, A. K. Singh, and B. I. Yakobson, J. Phys. Chem. C **115**, 9889 (2011).
168) Y. Liu, X. Wu, Y. Zhao, X. C. Zeng, and J. Yang, J. Phys. Chem. C **115**, 9442 (2011).
169) Y. Liu, S. Bhowmick, and B. I. Yakobson, Nano Lett. **11**, 3113 (2011).
170) L. Ci, L. Song, C. Jin, D. Jariwala, D. Wu, Y. Li, A. Srivastava, Z. F. Wang, K. Storr, L. Balicas, F. Liu, and P. M. Ajayan, Nat. Mater. **9**, 430 (2010).
171) J. Lu, K. Zhang, X. F. Liu, H. Zhang, T. C. Sum, A. H. Castro Neto, and K. P. Loh, Nat. Commun. **4**, 2681 (2013).
172) Y. Kobayashi, S. Mori, Y. Maniwa, and Y. Miyata, Nano Res. **8**, 3261 (2015).

Ryo Kitaura was born in Hyogo Prefecture, Japan in 1974. He obtained B.E. (1998) degree from Osaka Prefecture University, M.E. (2000) and Ph.D. (2003) degrees from Kyoto University. He worked as an assistant professor from 2005 and as an associate professor from 2008 at Faculty of Science, Nagoya University. He has worked on growth, structural characterization and electronic and optical properties of low dimensional materials including one- and two-dimensional materials such as carbon nanotubes, nanopeapods, nanowires, graphene, and transition metal dichalcogenides.

Yasumitsu Miyata was born in Kumamoto Prefecture, Japan in 1980. He obtained his B.Sc. (2004), M.Sc. (2006), and Ph.D. (2008) degrees from Tokyo Metropolitan University. He was an assistant professor (2009–2013) at Research Center for Materials Science, Nagoya University. Since 2013 he has been an associate professor at Graduate School of Science and Engineering, Tokyo Metropolitan University. He has worked on growth, structure control, and characterization of low-dimensional materials including graphene, boron nitride, transition metal dichalcogenides, and carbon nanotubes.

Rong Xiang was born in Anhui Prefecture, China in 1982. He obtained his B.Sc. (2003) from University of Science and Technology of China, M.Eng. (2006) from Tsinghua University, and Ph.D. (2009) degrees from the University of Tokyo. Since 2014 he has been an assistant professor at Graduate School of Engineering, the University of Tokyo. He has worked on controlled synthesis of low dimensional nano-carbon materials, including carbon nanotube and graphene.

James Hone recieved his B.S. from Yale University in 1990, and Ph.D. from California (Berkeley) in 1998. He is a Professor of Mechanical Engineering, Columbia Univeristy. He has worked on carbon nanotubes, nano-bioscience, and nanoelectromechanical systems (NEMS).

Jing Kong received her B.S. from Peking University in 1997 and the Ph.D. in chemistry from Stanford University in 2002. She worked as a research scientist at NASA Ames Research Center and a postdoctoral researcher at Delft University. She joined the MIT faculty in 2004 in the Department of Electrical Engineering and Computer Science. Her current research focuses on synthesis and characterization of two-dimensional materials.

Rodney S. Ruoff received his B.S. in chemistry from University of Texas-Austin in 1981 and Ph.D. in chemical physics from University of Illinois-Urbana in 1988. After working as a Postdoctoral Fellow at the Max Plancl Institute fuer Stroemungsforschung and the IBM-Watson Research Laboratory, he worked as a research staff scientist at the Molecular Physics Laboratory at SRI International. He moved to Washington University in 1997 and then became a full professor at Northwestern University in 2000, and a Cockrell Family Chair Professor at The University of Texas at Austin in 2007. He is now an IBS center director (the Center for Multidimensional Carbon) and Distinguished Professor at the Ulsan National Institute of Science and Technology, Korea. His current research focuses on design, synthesis, and characterization of new carbon and related materials. Please further note: https://en.wikipedia.org/wiki/Rodney_S._Ruoff.

Shigeo Maruyama was born in Tochigi Prefecture, Japan in 1960. He received Ph.D. in School of Engineering from the University of Tokyo in 1988. He worked as a research associate until 1991, as a lecturer for a year, as an associate professor from 1993, as a full professor from 2004, and as a distinguished professor from 2014 at the University of Tokyo. From April 2015, he also works as a cross-appointment fellow for Advanced Industrial Science and Technology (AIST). He invented the new CVD technique of SWNTs from low pressure alcohol in 2002, so-called Alcohol Catalytic CVD (ACCVD). His current research topics are growth, optical characterization, thermal characterization and solar cell application of carbon nanotubes and graphene.